J|A|C|S
ARTICLES
Published on Web 12/22/2005

Quenching of Fluorophore-Labeled DNA Oligonucleotides by Divalent Metal Ions: Implications for Selection, Design, and Applications of Signaling Aptamers and Signaling Deoxyribozymes

Nicholas Rupcich,[†] William Chiuman,[‡] Razvan Nutiu,[†] Shirley Mei,[‡] Kulwinder K. Flora,[†] Yingfu Li,*[,†,‡] and John D. Brennan*[,†]

Contribution from the Department of Chemistry, McMaster University, Hamilton, Ontario, Canada L8S 4M1, and Department of Biochemistry and Biomedical Sciences, McMaster University, Hamilton, Ontario, Canada L8N 3Z5

Received May 22, 2005; E-mail: brennanj@mcmaster.ca

Abstract: Recent years have seen a dramatic increase in the use of fluorescence-signaling DNA aptamers and deoxyribozymes as novel biosensing moieties. Many of these functional single-stranded DNA molecules are either engineered to function in the presence of divalent metal ion cofactors or designed as sensors for specific divalent metal ions. However, many divalent metal ions are potent fluorescence quenchers. In this study, we first set out to examine the factors that contribute to quenching of DNA-bound fluorophores by commonly used divalent metal ions, with the goal of establishing general principles that can guide future exploitation of fluorescence-signaling DNA aptamers and deoxyribozymes as biosensing probes. We then extended these studies to examine the effect of specific metals on the signaling performance of both a structure-switching signaling DNA aptamer and an RNA-cleaving and fluorescence-signaling deoxyribozyme. These studies showed extensive quenching was obtained when using divalent transition metal ions owing to direct DNA−metal ion interactions, leading to combined static and dynamic quenching. The extent of quenching was dependent on the type of metal ion and the concentration of supporting monovalent cations in the buffer, with quenching increasing with the number of unpaired electrons in the metal ion and decreasing with the concentration of monovalent ions. The extent of quenching was independent of the fluorophore, indicating that quenching cannot be alleviated simply by changing the nature of the fluorescent probe. Our results also show that the DNA sequence and the local secondary structure in the region of the fluorescent tag can dramatically influence the degree of quenching by divalent transition metal ions. In particular, the extent of quenching is predominantly determined by the fluorophore location with respect to guanine-rich and duplex regions within the strand sequence. Examination of the effect of both the type and concentration of metal ions on the performance of a fluorescence-signaling aptamer and a signaling deoxyribozyme confirms that judicious choice of divalent transition metal ions is important in maximizing signals obtained from such systems.

Introduction

DNA aptamers and deoxyribozymes (also known as catalytic DNAs, DNA enzymes, or DNAzymes) are two classes of single-stranded DNA molecules that have ligand-binding ability and catalytic function, respectively.[1−10] These artificial DNA molecules are isolated from random-sequence DNA pools by a technique known as SELEX or in vitro selection.[11,12] Many standard or modified DNA aptamers are now available for binding numerous targets ranging from metal ions to small molecule metabolites to proteins.[3,13,14] Similarly, there are a large number of catalytic DNA molecules that exist for the catalysis of many different chemical transformations.[1,6−9,15−18] Remarkably, recent years have seen a flurry of activity in exploiting DNA aptamers and deoxyribozymes for a variety of innovative

* Contact J.D.B. for fluorescence correspondence, and Y.L. for aptamer correspondence.
[†] Department of Chemistry.
[‡] Department of Biochemistry and Biomedical Sciences.

(1) Breaker, R. R. *Curr. Opin. Chem. Biol.* **1997**, *1*, 26−31.
(2) Famulok, M. *Curr. Opin. Struct. Biol.* **1999**, *9*, 324−329.
(3) Famulok, M.; Mayer, G.; Blind, M. *Acc. Chem. Res.* **2000**, *33*, 591−599.
(4) Osborne, S. E.; Matsumura, I.; Ellington, A. D. *Curr. Opin. Chem. Biol.* **1997**, *1*, 5−9.
(5) Rimmele, M. *Chembiochem* **2003**, *4*, 963−971.
(6) Achenbach, J. C.; Chiuman, W.; Cruz, R. P.; Li, Y. *Curr. Pharm. Biotechnol.* **2004**, *5*, 321−336.
(7) Emilsson, G. M.; Breaker, R. R. *Cell. Mol. Life Sci.* **2002**, *59*, 596−607.
(8) Jaschke, A. *Curr. Opin. Struct. Biol.* **2001**, *11*, 321−326.
(9) Li, Y.; Breaker, R. R. *Curr. Opin. Struct. Biol.* **1999**, *9*, 315−323.
(10) Sun, L. Q.; Cairns, M. J.; Saravolac, E. G.; Baker, A.; Gerlach, W. L. *Pharmacol. Rev.* **2000**, *52*, 325−347.
(11) Ellington, A. D.; Szostak, J. W. *Nature* **1990**, *346*, 818−822.
(12) Tuerk, C.; Gold, L. *Science* **1990**, *249*, 505−510.
(13) Lu, Y.; Liu, J.; Li, J.;, Bruesehoff, P. J.; Pavot, C. M. B., Brown, A. K. *Biosens. Bioelectron.* **2003**, *18*, 529−540.
(14) Wilson, D. S.; Szostak, J. W. *Annu. Rev. Biochem.* **1999**, *68*, 611−647.
(15) Joyce, G. F. *Annu. Rev. Biochem.* **2004**, *73*, 791−836.
(16) Breaker, R. R. *Science* **2000**, *290*, 2095−2096.
(17) Breaker, R. R. *Nat. Biotechnol.* **1997**, *15*, 427−431.
(18) Silverman, S. K. *Org. Biomol. Chem.* **2004**, *2*, 2701−2706.

10.1021/ja053336n CCC: $33.50

applications ranging from gene therapeutics to biosensing.[3,5−7,10,19−24] For example, various fluorescence-signaling aptamers have been developed as sensing probes for analysis of metabolites and proteins.[24−35] Likewise, various catalytic DNA systems have been established for the detection of chemical and biochemical entities through catalysis-promoted fluorescent signal generation.[13,23,36−42]

Standard DNA does not contain any intrinsic fluorescent groups that are amenable to the development of fluorescent sensors. However, aptamers and deoxyribozymes can be easily modified with external fluorophores to provide opportunities for fluorescence sensing. Many modification methods have been described,[43] which include attaching a fluorophore onto an aptamer,[25,26] engineering aptamer beacons,[29,44,45] the development of structure-switching DNA aptamers,[27,33] and the development of deoxyribozymes that synchronize fluorescence signaling with catalysis.[37] It is expected that signaling aptamers and deoxyribozymes will find increased uses in future bioanalytical applications, particularly considering the increasing availability of more and more DNA aptamers and deoxyribozymes, the convenience of selecting new aptamers and deoxyribozymes by in vitro selection, the ability to modify aptamers and deoxyribozymes with a wide array of fluorophores and quenchers, and the high chemical stability and ease of synthesis of DNA.

It is well-known that DNA duplex stability is related to ionic strength; relatively high ionic strength is necessary for proper charge screening of the negatively charged phosphate backbone to promote the stable formation of the DNA duplex. The negatively charged phosphodiester backbone of DNA also necessitates the need to use metal ions to promote proper folding of both aptamers and deoxyribozymes. Numerous reports cite the use of transition metal ions for this purpose, and metal ions that have been widely used include Mg(II), Ca(II), Mn(II), Co(II), Ni(II), Cu(II), Zn(II), and Cd(II).[36,46] Divalent metal ions are also implicated in some of the reaction mechanisms of ribozymes and deoxyribozymes.[47] Because of their importance to the function of both aptamers and deoxyribozymes, divalent metal ions have been widely utilized in selection buffers to assist the isolation of aptamers and deoxyribozymes, including signaling aptamers and deoxyribozymes. However, many divalent metal ions, particularly divalent transition metal ions, are potent fluorescence quenchers. Because of this, the sensitivity and selectivity of signaling aptamer or deoxyribozyme sensors will clearly depend on the extent of quenching of fluorescence by the divalent metal ions that are required for the optimal function of a DNA aptamer or a deoxyribozyme. Given that a key goal in the design of signaling aptamers and deoxyribozymes is to obtain maximum signaling efficiency, it is clear that the nature of the fluorophore tag, its location within the DNA sequence, and the nature of the metal ions present in the reaction buffer should all be optimized to minimize fluorescence quenching while at the same time promoting proper folding of the aptamer or deoxyribozyme to maximize target binding and/or catalytic performance. At present, there are no general rules to guide the engineering of optimal divalent metal ion-dependent fluorescence-signaling aptamers and deoxyribozymes. The development of such guidelines is a fundamental goal of this study.

The modes of metal-ion binding to DNA are numerous and have been described in detail by Izatt et al.[48] Metal ions coordinate with DNA bases at several sites, most notably at the N_7 of guanosine residues; metal ions also bind DNA through electrostatic interactions with the anionic phosphate backbone. Transition metal ions generally have different affinities for these sites, usually dictated by their valence and coordination geometry. In the case of fluorescence-signaling aptamers and deoxyribozymes, the presence of divalent metal ions may have severe implications on fluorescence emission. Transition metal ions are well-known as fluorescence quenchers and work via numerous mechanisms, including ground-state complexation,[49] collisional conversion of electronic to kinetic energy,[50] heavy-atom effects,[51] magnetic perturbations,[52,53] charge-transfer phenomena,[54] electronic energy transfer,[55] and fluorescence resonance energy transfer.[56] Normally, transition metal ions are rarely present at concentrations above 5 mM, reducing their

(19) Brody, E. N.; Gold, L. *J. Biotechnol.* **2000**, *74*, 5−13.
(20) Famulok, M.; Blind, M.; Mayer, G. *Chem. Biol.* **2001**, *8*, 931−939.
(21) Hesselberth, J.; Robertson, M. P.; Jhaveri, S.; Ellington, A. D. *J. Biotechnol.* **2000**, *74*, 15−25.
(22) Achenbach, J. C.; Nutiu, R.; Li, Y. *Anal. Chim. Acta* **2004**, *534*, 41−51.
(23) Nutiu, R.; Billen, L. P.; Li, Y. *Fluorescence-Signaling Nucleic Acid-Based Sensors*; Landesbioscience (in press): Weblink: http://www.eurekah.com/abstract.php?chapid=2191&bookid=169&catid=54, 2005.
(24) Nutiu, R.; Li, Y. *Chem.*−*Eur. J.* **2004**, *10*, 1868−1876.
(25) Jhaveri, S.; Kirby, R.; Conrad, R.; Maglott, E.; Bowser, M.; Kennedy, R. T.; Glick, G.; Ellington, A. D. *J. Am. Chem. Soc.* **2000**, *122*, 2469−2473.
(26) Jhaveri, S.; Rajendran, M.; Ellington, A. D. *Nat. Biotechnol.* **2000**, *18*, 1293−1297.
(27) Nutiu, R.; Li, Y. *J. Am. Chem. Soc.* **2003**, *125*, 4771−4778.
(28) (a) Nutiu, R.; Li, Y. *Angew. Chem., Int. Ed.* **2005**, *44*, 1061−1065. (b) Nutiu, R.; Yu, J.; Li, Y. *Chembiochem* **2004**, *5*, 1139−1144. (c) Nutiu, R.; Li, Y. *Angew. Chem., Int. Ed.* **2005**, *44*, 5464−5467.
(29) Hamaguchi, N.; Ellington, A.; Stanton, M. *Anal. Biochem.* **2001**, *294*, 126−131.
(30) Merino, E. J.; Weeks, K. M. *J. Am. Chem. Soc* **2003**, *125*, 12370−12371.
(31) Potyrailo, R. A.; Conrad, R. C.; Ellington, A. D.; Hieftje, G. M. *Anal. Chem.* **1998**, *70*, 3419−3425.
(32) Stojanovic, M. N.; de Prada, P.; Landry, D. W. *J. Am. Chem. Soc.* **2000**, *122*, 11547−11548.
(33) Stojanovic, M. N.; de Prada, P.; Landry, D. W. *J. Am. Chem. Soc.* **2001**, *123*, 4928−4931.
(34) Stojanovic, M. N.; Kolpashchikov, D. M. *J. Am. Chem. Soc.* **2004**, *126*, 9266−9270.
(35) Yamana, K.; Ohtani, Y.; Nakano, H.; Saito, I. *Bioorg. Med. Chem. Lett* **2003**, *13*, 3429−3431.
(36) Liu, Z.; Mei, S. H.; Brennan, J. D.; Li, Y. *J. Am. Chem. Soc.* **2003**, *125*, 7539−7545.
(37) (a) Mei, S. H.; Liu, Z.; Brennan, J. D.; Li, Y. *J. Am. Chem. Soc.* **2003**, *125*, 412−420. (b) Shen, Y.; Brennan, J. D.; Li, Y. *Biochemistry* **2005**, *44*, 12066−12076.
(38) Stojanovic, M. N.; Stefanovic, D. *Nat. Biotechnol.* **2003**, *21*, 1069−1074.
(39) Liu, J.; Lu, Y. *J. Am. Chem. Soc.* **2003**, *125*, 6642−6643.
(40) Liu, J.; Lu, Y. *Anal. Chem* **2003**, *75*, 6666−6672.
(41) Li, J.; Lu, Y. *J. Am. Chem. Soc.* **2000**, *122*, 10466−10467.
(42) Okumoto, Y.; Ohmichi, T.; Sugimoto, N. *Biochemistry* **2002**, *41*, 2769−2773.
(43) (a) Suljak, S. W.; Cao, Z.; Tan, W. *Recl. Res. Dev. Chem.* **2003**, *1*, 59. (b) Nutiu, R.; Mei, S.; Liu, Z.; Li, Y. *Pure Appl. Chem.* **2004**, *76*, 1547.
(44) Tyagi, S.; Kramer, F. R. *Nat. Biotechnol.* **1996**, *14*, 303−308.
(45) Yamamoto, R.; Baba, T.; Kumar, P. K. *Genes Cells* **2000**, *5*, 389−396.
(46) (a) Mondragon-Sanchez, J. A.; Liquier, J.; Shafer, R. H.; Taillandier, E. *J. Biomol. Struct. Dyn.* **2004**, *22*, 365−373. (b) Zimmermann, G. R.; Wick, C. L.; Shields, T. P.; Jenison, R. D.; Pardi, A. *RNA* **2000**, *6*, 659−667. (c) Kawakami, J.; Imanaka, H.; Yokota, Y.; Sugimoto, N. *J. Inorg. Biochem.* **2000**, *82*, 197−206.
(47) (a) Wrzesinski, J.; Ciesiolka, J. *Biochemistry* **2005**, *44*, 6257−6268. (b) Zivarts, M.; Liu, Y.; Breaker, R. R. *Nucleic Acids Res.* **2005**, *33*, 622−631. (c) Kuzuya, A.; Mizoguchi, R.; Komiyama, M. *Nucleic Acids Mol. Biol.* **2004**, *13*, 173−187.
(48) Izatt, R. M.; Christensen, J. J.; Rytting, J. H. *Chem. Rev.* **1971**, *71*, 439−481.
(49) Rutter, W. J. *Acta Chem. Scand.* **1958**, *12*, 438.
(50) Penzer, G. R.; Radda, G. K. *Quart. Rev. Chem. Soc.* **1967**, *21*, 43−65.
(51) Lower, S. K.; El-Sayed, M. A. *Chem. Rev.* **1966**, *66*, 199−241.
(52) Yuster, P.; Weissman, S. I. *J. Chem. Phys.* **1949**, *17*, 1182−1188.
(53) Brocklehurst, B. *Res. Rev.* **1970**, *2*, 149.
(54) (a) De Costa, M. D. P.; Jayasinghe, W. A. P. A. *J. Photochem. Photobiol. A: Chem.* **2004**, *162*, 591−598. (b) Hariharan, C.; Vijaysree, V.; Mishra, A. K. *J. Lumin.* **1997**, *75*, 205−211.
(55) (a) Bregadze, V.; Khutsishvili, I.; Chkhaberidze, J.; Sologhashvili, K. E. *Inorg. Chim. Acta* **2002**, *339*, 145−159. (b) Guarino, A.; Possagno, E.; Bassanelli, R. *J. Chem. Soc., Faraday Trans. 1* **1980**, *76*, 2003−2010.

effects on fluorescence intensity. However, fluorescently labeled DNA systems are unique because not only do transition metal ions interact with extrinsic fluorophores via the aforementioned mechanisms but they also interact with the DNA, creating a "preconcentration" effect that could lead to severe quenching even at low millimolar concentrations of metal ions. To minimize such effects, it is vital to consider the choice of metal ions to be included in the selection buffer from which a signaling aptamer or deoxyribozyme is isolated.

Herein we studied the effects of divalent transition metal ions on the fluorescence of several fluorescently labeled DNA oligonucleotides and probed the secondary structural features of oligonucleotides that can contribute to quenching. On the basis of our findings, we provide guidelines on the optimal selection of metal ions as well as on the selection of the optimal sequence and structure to which fluorophores are attached to minimize quenching in signaling aptamers and deoxyribozymes. We have also examined the effect of the type and concentration of metal ions on the performance of both a fluorescence-signaling aptamer and a fluorescence-signaling deoxyribozyme. The results show that the data from the quenching studies correlate well with the predicted effects of the different metals on the signaling levels from these species. From this, it is concluded that minimizing the concentration of divalent transition metal ions and maximizing ionic strength using monovalent ions are important in maximizing signals obtained from fluorescence-signaling aptamers and deoxyribozymes.

Experimental Section

Chemicals and DNA Oligonucleotides: All fluorophore-labeled oligonucleotides were prepared by automated DNA synthesis using cyanoethylphosphoramidite chemistry (Keck Biotechnology Resource Laboratory, Yale University) and purified by reversed-phase HPLC as described elsewhere.[27,37] The 5′-terminal fluorescein and internal fluorescein within each relevant DNA oligonucleotides were introduced during automated DNA synthesis using 5′-fluorescein phosphoramidite and fluorescein-dT amidite (Glen Research, Sterling, Virginia), respectively. The sequences of all oligonucleotides are depicted in the relevant figures, often with the drawing of potential secondary structures. Tris buffer, $MnCl_2 \cdot 4H_2O$, NaCl, and fluorescein were obtained from Sigma (Oakville, ON). $MgCl_2 \cdot 6H_2O$ and $CaCl_2$ were purchased from Fisher Scientific. $CoCl_2 \cdot 6H_2O$ and $CdCl_2 \cdot 5H_2O$ were acquired from Anachemia, and $NiCl_2 \cdot 6H_2O$ was purchased from Caledon. Water was purified with a Milli-Q Synthesis A10 water purification system. All other chemicals and solvents used were of analytical grade.

Procedures. Absorbance Measurements: Absorbance spectra of the DNA samples in the presence and absence of the divalent metal ions studied were collected on a Cary 400 UV/vis spectrophotometer operated in double-beam mode. Scans were collected in a small volume quartz cuvette with 1 cm path length from 240 to 600 nm using a scan rate of 200 nm/min.

Fluorescence-Quenching Measurements: Fluorophore-labeled DNA samples (FDNA1−3) were titrated with a range of divalent metal ions, including Mn(II), Mg(II), Ca(II), Co(II), Cd(II), and Ni(II). In all cases, samples were excited at 475 nm, and emission spectra were collected from 500 to 600 nm at a 600 nm/min scan rate using a Cary Eclipse spectrofluorimeter. Samples were not deoxygenated prior to testing, and titrations were run using continuous stirring to final concentrations of 250 μM of metal ion. The labeled DNA samples were placed in small volume quartz cuvettes at an initial concentration of 80 nM in 10 mM Tris buffer, pH 7.8 containing either 10 mM NaCl or 500 mM NaCl. Subsequent additions of the various metals were made from a 10 mM stock in the respective buffer. All emission intensity data were obtained by integrating the emission spectrum and were dilution corrected. The data were fit using the Stern−Volmer equation shown below:

$$\frac{F_0}{F} = 1 + k_q \tau_0 [Q] = 1 + K_{SV}[Q] \quad (1)$$

where F_0 and F are the fluorescence intensity in the absence and presence of a quencher, respectively; k_q is the bimolecular quenching constant; τ_0 is the lifetime of the fluorophore in the absence of quencher; [Q] is the molar concentration of the quencher, and K_{SV} is the Stern−Volmer quenching constant in M^{-1}.

Titrations were performed for FDNA3, the G-rich duplex mutant FDNA4, and the G-rich nonduplex forming mutant FDNA5 using Ni(II) as the test ion at room temperature (~20 °C) and 70 °C, which is well above the melting temperature of any of the anticipated potential duplex structures to ensure that changes in quenching were related to alterations in DNA structure. Quenching data were fit to eq 1, and differences in K_{SV} values were used to assess whether structural features influenced quenching.

Time-Resolved Fluorescence Measurements: Time-resolved fluorescence intensity decay data were acquired in the time domain using an IBH 5000U time-correlated single photon counting fluorimeter operated in the reverse mode. Light from a pulsed light-emitting diode operating at a 1 MHz repetition rate with a 1.3 ns pulse duration and a wavelength of 495 nm was passed through a single grating monochromator (32 nm band-pass) and a 500 nm short-pass filter and directed into a standard 1 cm quartz cuvette containing the sample. The fluorescence intensity decay data were collected at a right angle to the excitation path using magic angle polarization. Emitted photons were passed through a 515 nm long-pass emission filter used in combination with a single grating monochromator (32 nm band-pass) and detected using an IBH TBX-04 PMT. Data were collected into 4096 channels (12.2 ps/channel) using a multichannel acquisition card and analyzed using a discrete multiexponential decay model with DAS 6.0 fitting software provided by IBH.

Fluorescence-Quenching Assays of Structure-Switching Signaling Aptamer: FDNA6 (20 pmol) and QDNA (40 pmol) were mixed in ddH_2O in a total volume of 395 μL and heated at 90 °C for 3 min. The mixture was cooled to room temperature, and 100 μL of 5× assaying buffer (1× assaying buffer = 50 mM HEPES, pH 7.0, 300 mM NaCl, and 5 mM $MgCl_2$) was added to facilitate the hybridization between FDNA6 and QDNA. The solution was then incubated overnight at room temperature. In the case where the fluorescence-quenching profile of the signaling aptamer in the presence of supplementary M^{2+} (either Cd^{2+}, Co^{2+}, Ni^{2+}, Mg^{2+}, or Mn^{2+}) was to be probed, the relevant M^{2+} was also included at the designated concentrations in the overnight incubation. The fluorescence signals were recorded on a Cary Eclipse fluorescence spectrophotometer with excitation at 490 nm and emission at 520 nm. Background signals were determined from the fluorescence outputs of 1× assaying buffer and subtracted from the sample readings before F/F_0 was computed. Other information is given in the figure legend of relevant figures.

Fluorescence-Quenching Assays of Signaling Deoxyribozyme: Real-time signaling of DET22-18 in the presence of various Co^{2+} concentrations was conducted using a mixture containing 0.1 μM substrate and 1 μM deoxyribozyme in the presence of 1× reaction buffer containing 50 mM HEPES (pH 6.8 at 23 °C), 400 mM NaCl, 100 mM KCl, and $CoCl_2$ at 0.5, 1, 2, or 10 mM. For the first 10 min, each reaction mixture contained only substrate and all metal ions. Right after the 10th minute, the deoxyribozyme was added into the solution. Fluorescence intensity of each solution was recorded continuously at

(56) (a) Murphy, C. B.; Zhang, Y.; Troxler, T.; Ferry, V.; Martin, J. J.; Jones, W. E., Jr. *J. Phys. Chem. B* **2004**, *108*, 1537−1543. (b) Salthammer, T.; Dreeskamp, H.; Birch, D. J. S.; Imhof, R. E. *J. Photochem. Photobiol. A: Chem.* **1990**, *55*, 53−62.

1 min intervals on a Cary Eclipse fluorescence spectrophotometer with excitation at 490 nm and emission at 520 nm. For the radioactivity assay, 5′-^{32}P-labeled substrate (0.1 μM) was first mixed with the deoxyribozyme (1 μM), followed by the addition of the reaction buffer containing various concentrations of $CoCl_2$ (high concentration of stocks were used to achieve the final 1× concentration). Each reaction was stopped after 10 s with the addition of quenching buffer (30 mM EDTA and 8 M urea). The 5′-cleavage product was separated from uncleaved substrate by 10% denaturing PAGE. Percent cleavage was quantified using a PhosphorImager and ImageQuant software as previously described.[37]

Results and Discussion

Effect of Metal Ion on Quenching: Preliminary experiments were done to assess the degree of quenching of a series of fluorescein-labeled DNA samples by different divalent metal ions. Fluorescein was chosen owing to its widespread use in the development of fluorescence-signaling aptamers[18,24−28,33,34,45,57] and deoxyribozymes.[36,37] Quenching studies were also done using other fluorophores conjugated to DNA, including Cy3, Cy3.5, rhodamine, Alexafluor 488, and Alexafluor 546. While there were minor differences in the quenching behavior of the various FDNA samples (data not shown), the trends observed for fluorescein were also observed for the other probes. Thus, alleviation of quenching cannot be achieved simply by changing the nature of the fluorescent probe. The metal cations were selected due to their prominent use in deoxyribozyme selection protocols[6,36,37,58−65] and also to examine any trends that may exist among their differing electronic valence configurations.

As shown in Figure 1, the degree of quenching, as determined by the K_{SV} value, was dependent on both the nature of the metal ion and the sequence of the DNA strand. Issues related to the effects of DNA sequence on the extent of quenching are discussed in more detail below. Examining the effects of divalent metal ions, there was essentially no quenching from either Ca(II) or Mg(II) (data not shown), which is expected given that these species are widely used in conjunction with fluorescence assays and have not been reported to quench fluorescence emission. On the other hand, the level of quenching by the remaining divalent cations was extremely high and was dependent on both the nature of the metal ion and the amount of NaCl in the supporting buffer, decreasing with increasing ionic strength. The high degree of quenching, coupled with the dependence on ionic strength, strongly argues for an electrostatic contribution to the overall quenching process. Indeed, as shown in Figure 1, the K_{SV} values obtained by Stern−Volmer analysis of quenching data are orders of magnitude higher than the theoretical diffusion-limited values that would be expected for purely collisional quenching (theoretical maximum K_{SV} for fluorescein is ∼60 M^{-1}).[66]

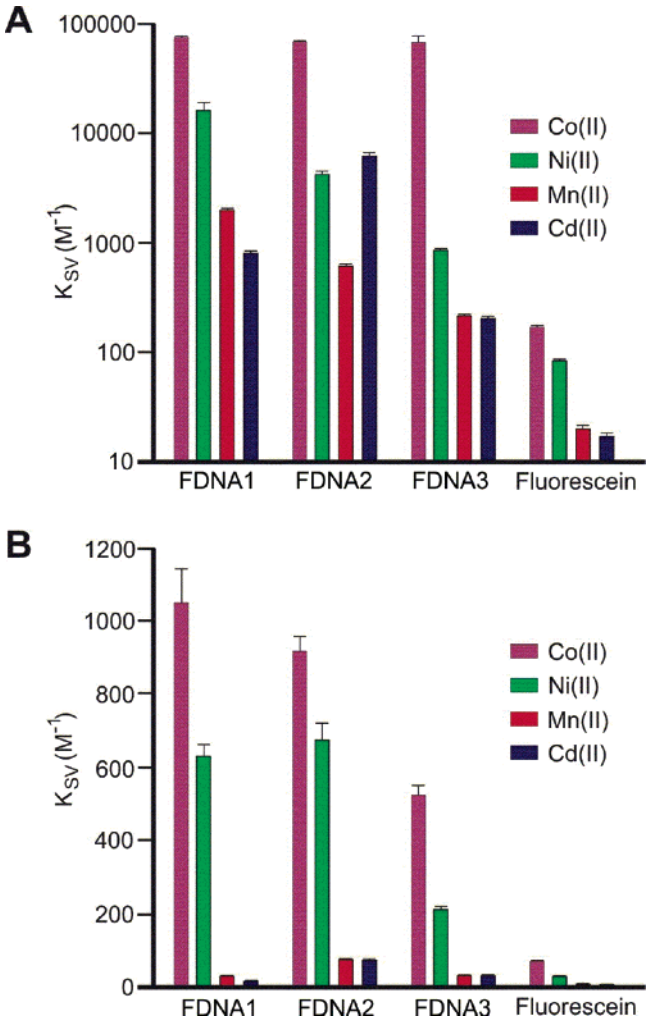

Figure 1. K_{SV} values for metal ion quenching of three 5′-fluorescein-labeled DNA oligonucleotides (FDNA1−3) in (A) 10 mM NaCl and (B) 500 mM NaCl buffers. Note that the *y*-axis in panel A is on a logarithmic scale, while that in panel B is on a linear scale.

The phosphate backbone of DNA and the DNA bases themselves offer several sites for metal ion coordination. These sites include coordination with the DNA bases alone or in conjunction with the deoxyribose or phosphate moieties.[48] Moldrheim et al. proposed that the binding of transition metal ions to DNA oligonucleotides is determined by (i) the nucleophilicity of the binding site and (ii) the coordination geometry of the metal ions.[67] Of these sites, the preferred binding site is the endocyclic nitrogen N_7 of guanine.[68]

Focusing on the dependence of quenching on the specific metal ion, it was generally observed that Co(II) was the most potent quencher, followed by Ni(II), Mn(II), and Cd(II). In terms of K_{SV} values, the four metal ions ranged from a high of 74 000 M^{-1} for Co(II) in 10 mM NaCl to a low of 200 M^{-1} for Cd(II) under similar ionic strength conditions. Put into perspective, a K_{SV} value of 74 000 M^{-1} translates to a 100-fold decrease in fluorescence intensity at a Co(II) concentration of only 1.35 mM (when using 10 mM NaCl), while a K_{SV} of 200 M^{-1} translates into only a 30% decrease in intensity at a similar

(57) Jiang, Y.; Fang, X.; Bai, C. *Anal. Chem.* **2004**, *76*, 5230−5235.
(58) Carmi, N.; Shultz, L. A.; Breaker, R. R. *Chem. Biol.* **1996**, *3*, 1039−1046.
(59) Cuenoud, B.; Szostak, J. W. *Nature* **1995**, *375*, 611−614.
(60) Li, J.; Zheng, W.; Kwon, A. H.; Lu, Y. *Nucleic Acids Res.* **2000**, *28*, 481−488.
(61) Li, Y.; Breaker, R. R. *Proc. Natl. Acad. Sci. U.S.A.* **1999**, *96*, 2746−2751.
(62) Li, Y.; Liu, Y.; Breaker, R. R. *Biochemistry* **2000**, *39*, 3106−3114.
(63) Schlosser, K.; Li, Y. *Biochemistry* **2004**, *43*, 9695−9707.
(64) Sreedhara, A.; Li, Y.; Breaker, R. R. *J. Am. Chem. Soc.* **2004**, *126*, 3454−3460.
(65) (a) Wang, W.; Billen, L. P.; Li, Y. *Chem. Biol.* **2002**, *9*, 507−517. (b) Achenbach, J. C.; Jeffries, G.; McManus, S.; Billen, L. P.; Li, Y. *Biochemistry* **2005**, *44*, 3765−3774.
(66) Lakowicz, J. R. *Principles of Fluorescence Spectroscopy*, 2nd ed.; Kluwer Academic: New York, 1999; pp 241−242.
(67) Moldrheim, E.; Andersen, B.; Froystein, N. A.; Sletten, E. *Inorg. Chim. Acta* **1998**, *273*, 41−46.
(68) Gao, Y.; Sriram, M.; Wang, A. J. *Nucleic Acids Res.* **1993**, *21*, 4093−4101.

concentration of Cd(II). In the case of Co(II), the quenching is roughly 1200-fold greater than what would be expected for purely diffusional quenching, suggesting an "effective concentration" of metal ion in the vicinity of the DNA that is 1200-fold higher than the bulk solution concentration. The decreasing pattern of K_{SV} values, which is most obvious for the 15-nt FDNA1, follows very closely with the number of unpaired d electrons in the divalent metal ion series. Co(II), Ni(II), Mn(II), and Cd(II) have five, four, three, and two unpaired electrons in their respective d shells. Thus the higher number of unpaired electrons present in the d shell of the transition metal ion causes more efficient quenching of the excited fluorophore by a charge-transfer mechanism.

In addition to charge-transfer quenching, the spectral properties of Co(II) make it possible for the DNA-linked fluorophore to undergo energy transfer into the $t_{2g} \rightarrow e_g$ absorbance band, which extends to nearly 600 nm. Similarly, Ni(II) and Mn(II) also have low $t_{2g} \rightarrow e_g$ splitting energies and thus fall in the category of weak-field ligands. Förster distances for fluorophore−Co(II) energy transfer has been reported to be relatively short (1.3−2.0 nm),[69,70] but still larger than the <1 nm distance necessary for static quenching. Thus Co(II) could potentially quench a DNA-bound fluorophore via FRET at distances double or triple that of the other metal ions in addition to collisional or static quenching mechanisms, inflating its quenching constant to the very high values observed.

To further assess the origins of the unusually high K_{SV} values, we used time-resolved fluorescence measurements to separate contributions to the overall quenching arising from static and dynamic quenching processes. In this case, lifetime data were fit to eq 2 to extract the dynamic quenching constant (K_D):

$$\frac{\tau_0}{\tau} = 1 + K_D[Q] \qquad (2)$$

The static quenching constant (K_S) was then calculated by combining K_D from the lifetime data with the intensity-based quenching data according to eq 3:

$$\frac{F_0}{F} = (1 + K_D[Q])(1 + K_S[Q]) \qquad (3)$$

Table 1 summarizes the intensity weighted mean lifetimes in the presence and absence of the metal ion quenchers as well as the calculated K_D and K_S values for free fluorescein and for various FDNAs as a function of ionic strength. Only data for Co(II) and Ni(II) quenching are shown since both Mn(II) and Cd(II) resulted in essentially no dynamic quenching of free fluorescein at the concentrations of metal ions employed in the study, indicating that the bulk of the quenching obtained using these metal ions could be attributed to static quenching. In general, it was observed that free dyes showed relatively consistent dynamic quenching constants, which were generally within the range expected for dynamic quenching. K_D values were somewhat higher for Co(II), presumably due to the higher number of unpaired d electrons relative to Ni(II), and decreased slightly with increased ionic strength. This trend, coupled with the nonzero static quenching constants for free fluorescein at low ionic strength, suggests the presence of weak binding interactions between the dianionic fluorescein and the metal ions.

Table 1. Lifetime Measurements and Dynamic versus Static Quenching Determination (error values are given in parentheses)

sample	$\langle\tau\rangle$ (ns)[a]	τ_0/τ[b]	K_D (M^{-1})	K_S (M^{-1})
fluorescein (10 mM NaCl)	3.96			
fluorescein + Co(II)	3.26	1.22	56 (3)	18 (1)
fluorescein + Ni(II)	3.54	1.12	31 (2)	11 (1)
fluorescein (500 mM NaCl)	3.94			
fluorescein + Co(II)	3.49	1.13	33 (2)	0
fluorescein + Ni(II)	3.75	1.05	13 (1)	0
FDNA2 (10 mM NaCl)	3.94			
FDNA2 + Co(II)	2.63	1.50	4089 (412)	19900 (2000)
FDNA2 + Ni(II)	2.76	1.42	621 (62)	2320 (230)
FDNA2 (500 mM NaCl)	4.04			
FDNA2 + Co(II)	2.77	1.46	139 (16)	6140 (708)
FDNA2 + Ni(II)	3.31	1.22	67 (4)	1600 (88)

[a] Typical errors in mean lifetimes are ±0.03 ns. [b] Typical errors in τ_0/τ values are ±0.02.

In the case of FDNA, the most striking change in quenching behavior relates to the large values of both K_D and K_S. Indeed, K_D values of approximately 4000 and 600 M^{-1}, respectively, are obtained at low ionic strength for Co(II) and Ni(II). These values are well above the expected limit established by the fluorescein control and are consistent with dynamic quenching not being dominated by a purely diffusion-based process. Given that the metal ions are preassociated with the DNA surrounding the fluorophore, it is likely that dynamic quenching is determined by short-range movement of the fluorophore and metal ions with respect to each other, possibly aided by "hopping" of metal ions along the DNA backbone.[71] The high K_S values relative to free fluorescein provide strong evidence for a direct interaction between the quencher and the fluorescently labeled DNA oligonucleotide.[66] The binding constants for Co(II) and Ni(II) to DNA are reported to be essentially equivalent,[48] thus the differences in K_S are likely due to more efficient quenching by Co(II) relative to Ni(II), consistent with the higher number of unpaired electrons in the former case. The direct interaction is further supported by the decreases in both K_D and K_S values for both metal ions as ionic strength increases. These data are in general agreement with the K_{SV} values and conclusively demonstrate direct quencher (metal ion)−DNA interactions.

Effect of DNA Sequence on Quenching: As noted above, the extent of quenching was dependent not only on the nature of the metal ion but also on the sequence of the DNA and the location of the fluorophore within the DNA sequence. In the absence of specific effects related to particular nucleotides or secondary structures, one would predict that quenching would initially increase with DNA strand length since more metal ions could bind to a longer DNA oligonucleotide, eventually reaching a maximum. According to Atherton et al., intercalated ethidium bromide can be quenched by metal ions bound to the DNA up to six phosphate backbone groups away from the fluorophore. They further proposed that the metal ions are mobile along the DNA strand, and that they can "hop" from base to base quite rapidly.[71] While these observations pertained to double-stranded DNA, they can bear importance to single-stranded DNA aptamers and deoxyribozyme whose secondary structure can contain segments of helical DNA.

(69) Birch, D. J. S.; Suhling, K.; Holmes, A. S.; Salthammer, T.; Imhof, R. E. *Pure Appl. Chem.* **1993**, *65*, 1687−1692.
(70) Horrocks, W. D.; Holmquist, B.; Vallee, B. L. *Proc. Natl. Acad. Sci. U.S.A.* **1975**, *72*, 4764−4768.
(71) Atherton, S. J.; Beaumont, P. C. *J. Phys. Chem.* **1986**, *90*, 2252−2259.

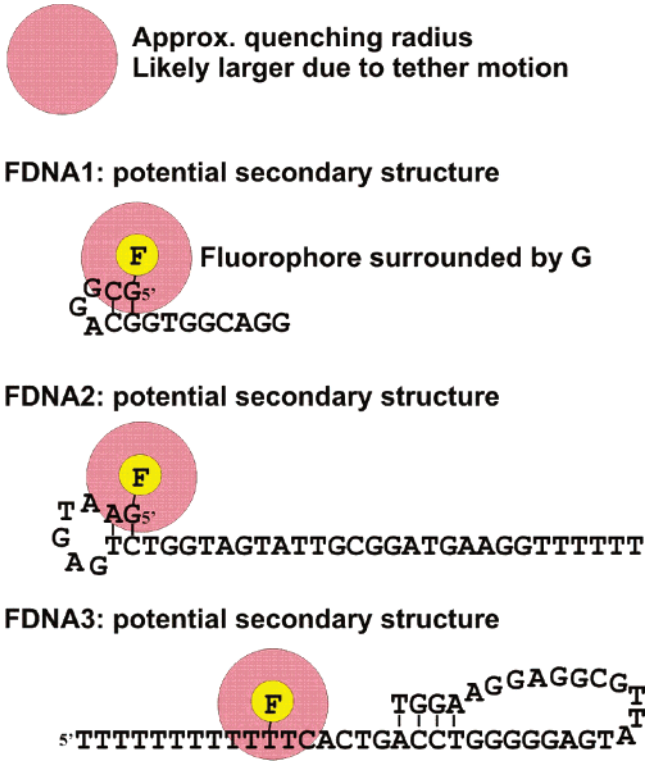

Figure 2. Secondary structures of FDNA1−3, depicted with the approximate quenching spheres of action around the fluorophore. All structures are those predicted at a temperature of 20 °C, where the quenching data were collected.

The variation in K_{SV} values for FDNAs of different length, shown in Figure 1, indicated that DNA strand length was not correlated to quenching efficiency, suggesting that other factors were responsible for the changes in quenching. Figure 2 depicts the probable secondary structures of the DNA sequences, as predicted by the mfold program.[72] Also portrayed is the approximate quenching sphere of action surrounding each fluorophore at its respective location. The approximation was made based on the sum of the radii of the metal ions and the fluorophore being on the order of 10 Å. Along its axis, DNA is approximately 3.3 Å in length per base, thus it is likely that metal ions bound up to three bases away from the fluorophore could quench via a static mechanism. This overlap of metal ion and fluorophore is likely an underestimation due to the flexibility of the fluorophore, which is bound to the DNA via a six-carbon tether.

Inspection of the sequences tested show that the three secondary structures and fluorophore locations within the structures vary greatly among the samples. While the 15-nt FDNA1 is the shortest strand, its sequence, structure, and fluorophore location situate the fluorophore adjacent to a duplex region that increases the anionic environment surrounding the fluorophore and attracts more metal ions. Additionally, the region in the immediate vicinity of the fluorophore is very guanine-rich (G-rich). Metal ions are known to preferentially bind to the N_7 of guanosine,[68] and thus this likely also creates a preconcentration of metal ions within the fluorophore quenching sphere. The 38-nt FDNA2 also situates the fluorophore near a duplex region. However, the number of G residues within the quenching sphere is less than that of FDNA1, and the duplex

(72) Zuker, M. *Nucleic Acids Res.* **2003**, *31*, 3406−3415.

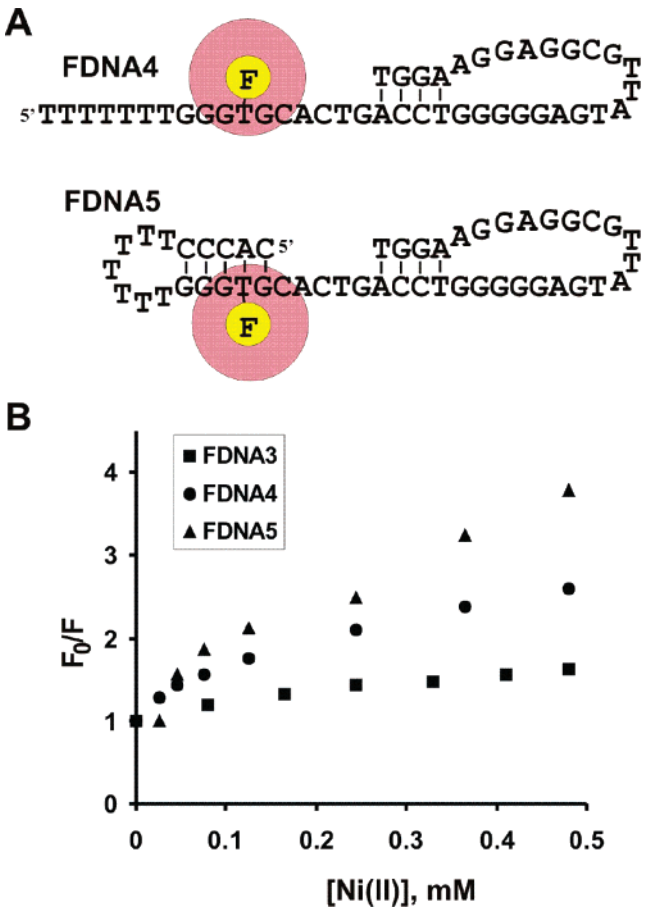

Figure 3. (A) FDNA4 and FDNA5 as two mutants of FDNA3 for assessment of increased quenching susceptibility. (B) Stern−Volmer plots of FDNA3−5.

is two bases removed from the fluorophore. Finally, the fluorophore location on the 44-nt FDNA3 is isolated from the duplex region and is tethered to a poly-T tail lacking nearby G residues, and indeed this sequence shows the lowest quenching of the three strands tested. On the basis of this simple analysis, it appears that the extent of quenching is predominantly determined by the fluorophore location with respect to G-rich and duplex regions within the strand sequence. DNA strand length may indirectly affect quenching since longer DNA strands are more likely to fold to give regions of secondary structure.

To further examine the effects of DNA sequence on quenching without complications related to strand length, we prepared two mutant sequences of FDNA3 designed to alter the G-content and secondary structure around the fluorophore. FDNA3 was chosen as the reference FDNA due to its relatively low quenching sensitivity, owing to the fluorophore position and lack of guanine residues near the fluorophore. The first mutant, FDNA4, replaced the thymine residues that surrounded the fluorophore with four guanosine residues. It was anticipated that this substitution would cause an increase in metal ion binding sites in the vicinity of the fluorophore. The second mutant, FDNA5, extended the size of the DNA oligonucleotide to 49 nucleotides and introduced 5 additional nucleotides which could form a stem loop with the G-rich sequence immediately surrounding the fluorophore. The probable secondary structures, as predicted by mfold, are shown in Figure 3A. Ni(II) was chosen to test the mutants for their susceptibility to quenching since it showed significant static quenching but had minimal

Table 2. K_{SV} Values of Oligonucleotides as a Function of Temperature (error values are given in parentheses)

sample	K_{SV} at 20 °C	K_{SV} at 70 °C
FDNA3	855 (25)	900 (32)
FDNA4 (G mutant of FDNA3)	7000 (430)	4990 (312)
FDNA5 (G duplex mutant of FDNA3)	14400 (1220)	5020 (286)

potential to participate in FRET-based quenching. Figure 3B shows the Stern−Volmer plots obtained from these oligonucleotides. The curves show downward curvature, indicative of saturation of the metal binding sites at higher concentrations of metals. K_{SV} values were approximated using the initial slope of the Stern−Volmer plots. As shown in Table 2, the introduction of a G-rich sequence surrounding the fluorophore increased the K_{SV} value from 855 M^{-1} for the original FDNA3 to 7050 M^{-1} for FDNA4. The second mutation, which extended FDNA4 to create a stem loop duplex at the fluorophore site, further increased the K_{SV} value to 14 400 M^{-1}. Thus, the expected effects of duplex structure and guanosine residues were confirmed.

To ensure that the variations in K_{SV} values were due to alterations in the structure of the DNA, quenching experiments were also performed on FDNA3−5 at a temperature that was above the melting temperature of the small duplex regions predicted by mfold. As shown in Table 2, heating of the DNA caused the observed K_{SV} values of the two mutants to become essentially identical, as expected, since in the absence of the hairpin duplex, the sequences immediately surrounding the fluorophore are identical. This result indicates the loss of the duplex region in the fluorophore vicinity, which was engineered to be intact at room temperature, and further supports the hypothesis that fluorophore location near DNA duplex regions enhances its sensitivity to transition metal quenching.

Effects of Metal Ions on Aptamer Signaling: On the basis of the above results, we decided to investigate the influences of divalent metal ions on the signaling performance of a previously characterized fluorescent DNA aptamer sensor for ATP detection (Figure 4A). The DNA aptamer, denoted FDNA6 in this report, is labeled with a fluorescein at its 5′-end and designed to form a DNA duplex structure with QDNA, a 12-nt DNA oligonucleotide with a DABCYL label (Q) placed at its 3′-end. In the absence of ATP, the duplex formation is expected to result in a very low level of fluorescence due to the fluorescence quenching by DABCYL. When ATP is added, the FDNA6/QDNA duplex will dissociate, with the concomitant formation of an FDNA6/ATP complex. The separation of QDNA from FDNA6 will lead to the generation of a fluorescence signal. First, we examined the quenching effects of Co(II), the most potent metal quencher from the results presented above. Mg(II) was chosen as the nonquenching control. It should be noted that all aptamer signaling assays were run in 1× assaying buffer containing 50 mM HEPES (pH 7.0), 300 mM NaCl, and 5 mM $MgCl_2$ (these conditions are required to maintain the aptamer activity), and thus the degree of quenching should be most similar to the value obtained in 500 mM NaCl (see Figure 1B). As shown in Figure 4B, the addition of Co(II) led to a concentration-dependent decrease in the relative signaling magnitude, which dropped from ∼5.5-fold in the absence of Co(II) to only 3.5-fold at 10 mM Co(II). In stark contrast, the addition of Mg(II) resulted in a concentration-dependent increase in signal enhancement from 5.5-fold to almost 7-fold (for clarity, only the data from 5 and 10 mM Mg are shown), consistent with the metal ion stabilizing the active structure of the aptamer. Comparing the final signal enhancements for 10 mM Co(II) and Mg(II), it is clear that the signaling efficiency dropped by a factor of 2, even at the relatively high ionic strength. Figure 4C shows the absolute fluorescence intensity of the aptamer prior to addition of ATP and demonstrates that the initial signal drops by a factor of 6.5 upon addition of 10 mM Co(II), while addition of 10 mM Mg(II) resulted in a loss of only 10% in signal. This translates to a need to use ∼6× more aptamer to generate the same baseline signal, or ∼12-fold more aptamer to generate the same final signal, when using 10 mM Co(II) relative to 10 mM Mg(II).

Figure 5 illustrates the effects of three other metal ions — Mn(II), Cd(II), and Ni(II)—on the fluorescence outputs of the same aptamer under the same assaying conditions. Panel A shows the fluorescence enhancement, upon ATP binding, when each metal ion (at 5 and 10 mM) was included in the initial signaling mixture; panel B plots the actual fluorescence intensity of each solution prior to ATP-induced structure switching. Briefly, Mn(II) produced a slight signal enhancement, similar to Mg(II). This was not unexpected based on the relatively low extent of quenching for this metal at high ionic strength. In contrast, Ni(II) exhibited an effect even beyond that obtained with Co(II), with the signal increasing by only a factor of 2. Surprisingly, Cd(II) caused a moderate decrease in signaling, although both Mn(II) and Cd(II) have similar quenching efficiencies. On the other hand, the data given in Figure 5B indicate that the baseline fluorescence intensities followed the expected trend, with Mn(II) and Cd(II) showing the least quenching, followed by Ni(II), and finally Co(II). This is in agreement with the K_{SV} values shown in Figure 1B. Taken together, these data imply that Ni(II) and likely also Cd(II) have some added effect, such as alteration of the active structure of the aptamer, which results in reduced signaling ability of the aptamer system (this speculation is further supported by the data presented in Figure 6). Thus, the role of metal ions goes beyond simple quenching, indicating that one must also consider structural roles played by metal ions.

Figure 6A shows the effects of all metal ions on the fluorescence output of aptamers with bound ATP. This experiment was meant to represent the situation where a sample containing both ATP and a metal ion is introduced to the aptamer after recording of a baseline signal. The effects of ATP and the metal are separated in time to better demonstrate the effects of each component on the final signal. As expected, addition of ATP resulted in a significant increase in the signal in the absence of metal (ca. 5.5-fold). However, addition of Co(II) and Ni(II) produced marked decreases in the signal in a concentration-dependent fashion (for clarity, only the data obtained with 5 and 10 mM metal ions are shown). Cd(II) caused significant but less dramatic decreases in fluorescence enhancement. Mn(II) produced a noticeable but small effect at 10 mM but had no effect at 5 mM. In contrast, the addition of both 5 and 10 mM Mg(II) raised the signaling magnitude, reflecting the fact that extra Mg(II) can stabilize the ATP-bound aptamer structure. As shown in Figure 6B, the final fluorescence intensity decreased drastically with addition of either 5 or 10 mM Co(II) or Ni(II). At 10 mM, these two metal ions suppressed the fluorescence to a level that was even lower than the initial

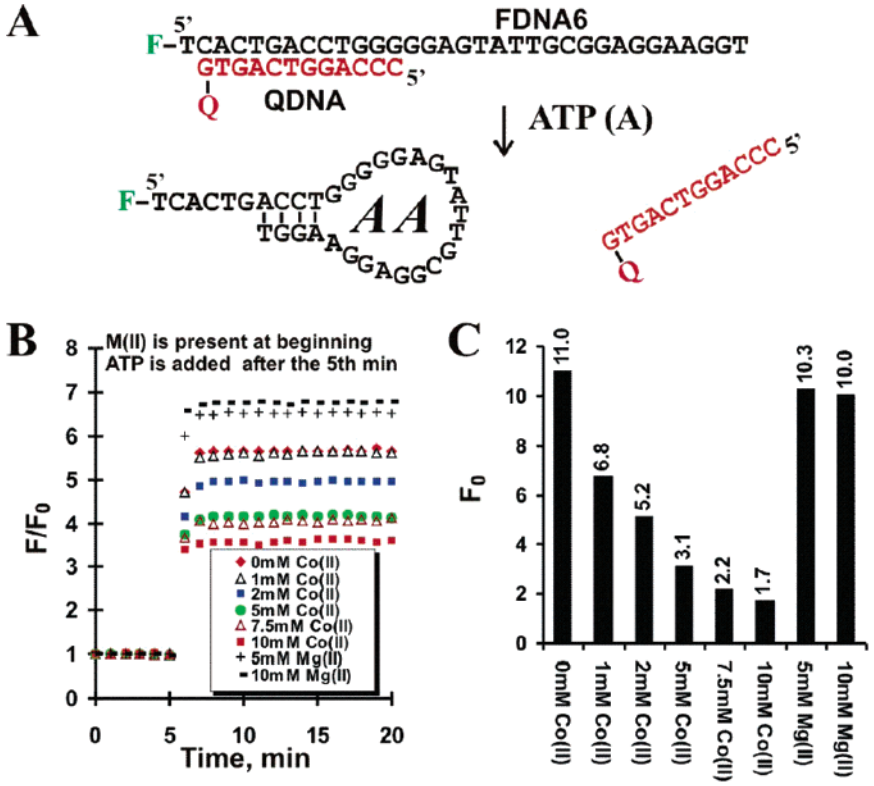

Figure 4. Effects of Co(II) and Mg(II) on fluorescence outputs of a known structure-switching signaling aptamer. (A) The design and signaling mechanism of the aptamer sensor for ATP. FDNA6 is an ATP-binding DNA aptamer labeled with a fluorescein (F) at its 5′-end. QDNA is a DNA oligonucleotide containing a DABCYL (Q) at its 3′-end. (B) Influence on the signaling capability by Co(II) and Mg(II) added at the duplex stage. FDNA6, QDNA, and Co(II) or Mg(II) in the 1× assaying buffer (see Experimental Section) was present at the beginning. ATP was introduced after 5 min of incubation. F, fluorescence intensity at a given time point; F_0, the initial fluorescence intensity (i.e., baseline fluorescence intensity). (C) The absolute value of F_0 of each sample corresponding to panel B.

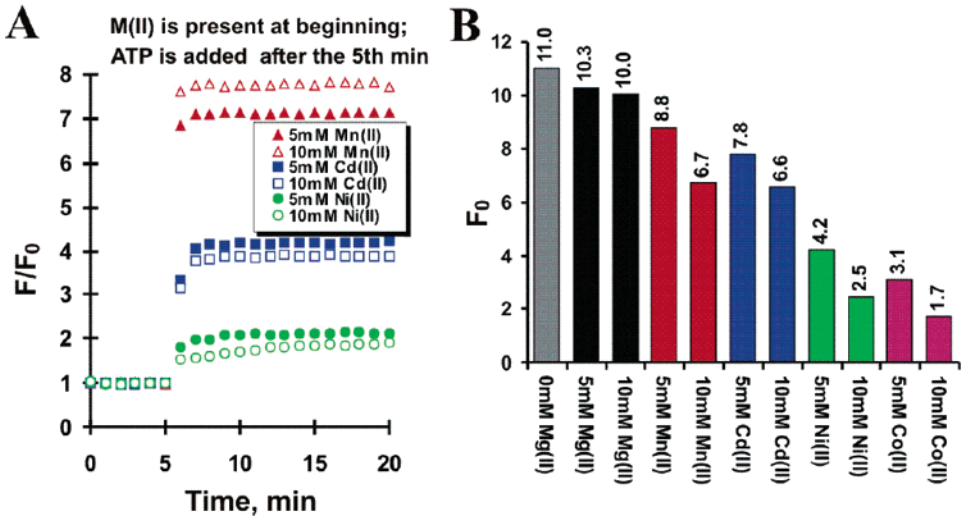

Figure 5. Effects on fluorescence outputs by Ni(II), Cd(II), and Mn(II) added at the duplex stage. (A) Influence by 5 and 10 mM of Ni(II), Cd(II), or Mn(II) introduced before ATP addition. Sample analysis is similar to the procedure described in the panel B of Figure 4. (B) The absolute value of F_0 of each sample corresponding to panel A.

intensity (recall that the signaling system had a baseline signal level of 11.0 units prior to addition of either ATP or metal ions; see Figure 4C). Cd(II) also caused a quite significant drop in fluorescence intensity. On the other hand, the final signal level of systems containing Mg(II) and Mn(II) remained high, showing that the signaling ability was retained in the presence of these two metal ions. Once again, the trend generally followed that expected based on K_{SV} values. Thus, when using highly quenching metal ions, such as Co(II), the final signal, relative to the unquenched baseline signal, can be positive, negative, or unchanged, depending on metal ion concentration. Since in practice the effects of ATP and metal ions would not be separable, one would not be able to accurately detect ATP using this system, particularly if the presence of the metal ion was unknown.

Finally, comparing the data presented in both Figure 5B and 6B leads to some interesting findings with regard to differential abilities of the metal ions to influence the signaling levels of

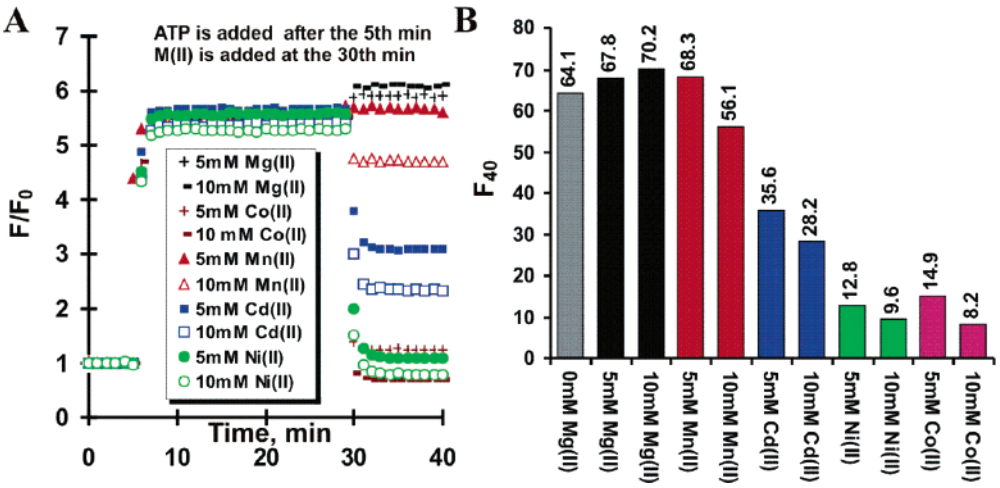

Figure 6. Effects on fluorescence signal by M(II) added at the complex stage. (A) Influences by 5 and 10 mM M(II) introduced after ATP addition. FDNA6 and QDNA in the 1X assaying buffer (see Experimental Section) were present at beginning. ATP was then introduced after 5 min of incubation. At the 30th minute, M(II) was added. (B) The absolute value of fluorescence of each sample in panel A at the 40th minute.

the signaling duplex (no ATP) and ATP-bound signaling complex. The potent quencher Co(II) caused very severe quenching to the intensity of both the duplex and complex. At the other end of the spectrum, Mg(II) caused very small suppression to the duplex signal but rendered a detectable enhancement to the complex signal. Most interestingly, Mn(II) and Cd(II) exhibited almost identical quenching to the duplex signal (Figure 5B), but their abilities in suppressing the complex signal were very different (Figure 6B). At 5 mM, Mn(II) worked to enhance the complex signal (most likely due to its ability to stabilize the complex formation); at 10 mM, this same metal functioned to suppress the complex signal (most likely due to its quenching effect). On the other hand, Cd(II) at both 5 and 10 mM produced much stronger suppression of the complex signal relative to the duplex signal, suggesting that Cd(II) may destabilize the complex structure. Denaturation of the complex structure also appeared to be the case for Ni(II) as it exhibited a level of quenching to the complex that was similar to Co(II)—the most potent quencher revealed by the K_{SV} data (Figure 1).

Taken together, the examples outlined above conclusively demonstrate the effects that various metal ions can have on aptamer signaling, both as a result of quenching of fluorescence and to some extent owing to structural roles played by the metals. Thus, it is important to recognize the importance of selecting or designing aptamers under conditions that minimize exposure to metals that can quench florescence. On the basis of these studies, the optimal metals for aptamer selection appear to be Mg(II) or possibly Mn(II) if used at levels of 10 mM or less. It is also important to ensure that samples to be tested for ATP are free from millimolar levels of transition metals such as Ni(II) and Co(II), as these cause extensive alterations in signaling behavior.

Effect of Metal Ion Concentration on Deoxyribozyme Signaling: Next, we chose to study the metal ion influence on the signaling properties of a second class of DNA-based fluorescent biosensor: signaling deoxyribozymes. More specifically, we sought to examine the influence of the concentration of Co(II) on signaling capability as well as the catalytic activity of DET22-18, a Co(II)-dependent, RNA-cleaving deoxyribozyme previously isolated by our groups in an in vitro selection experiment.[37] This deoxyribozyme (the green DNA strand in Figure 7A) cleaves a chimeric DNA/RNA substrate (the purple DNA strand) containing a single ribonucleotide (Ar: adenine ribonucleotide) as the cleavage site. More importantly, for fluorescence signaling, the ribonucleotide is immediately flanked by two thymine deoxyribonucleotides, one labeled with fluorophore and the other with DABCYL. The substrate in the uncleaved form has a low level of fluorescence. The addition of the deoxyribozyme in the presence of Co(II) will lead to the cleavage of the ribonucleotide and separation of F and Q. This is an intriguing system; on one hand, the signaling deoxyribozyme needs Co(II) as a cofactor to assist its catalytic activity and thus realize its signal generation function; on the other hand, Co(II) works against the generation of a high level of fluorescence due to its potent quenching ability. As expected, the initial increase of the Co(II) concentration from 0.5 to 1.0 mM led to a significant increase in signaling (Figure 7B), which reflected an increase in the extent of cleavage of the substrate by the deoxyribozyme. Further increases in Co(II) concentration (first to 2 mM and then to 10 mM) resulted in significant loss of signaling capability, consistent with the potent quenching ability of Co(II).

To demonstrate that the decrease of signaling was not due to the denaturation of the deoxyribozyme structure, we conducted gel electrophoresis analysis of the cleavage mixture of the 5′-^{32}P-labeled substrate (see embedded gel image in Figure 7C). The result clearly indicated an increase in the extent of cleavage when the Co(II) concentration was raised. Comparing 2 and 10 mM Co(II), the cleavage yield increased from 15 to ~40% (Figure 7C), while signaling magnitude decreased from ~10-fold to less than 4-fold (Figure 7B). Thus, the quenching of the signal by Co(II) mirrored that found above for the structure-switching aptamer, indicating again that high levels of Co(II) can drastically suppress fluorescence signaling. It should be noted that DET22-18 was selected in the presence of Co(II), thus this metal ion is required for efficient catalysis. Clearly, conducting in vitro selection experiments in the presence of alternative metal ions is necessary to maximize the signaling performance of deoxyribozyme biosensors.

Implications for Design and Selection of Signaling Aptamers and Signaling Deoxyribozymes: The results described

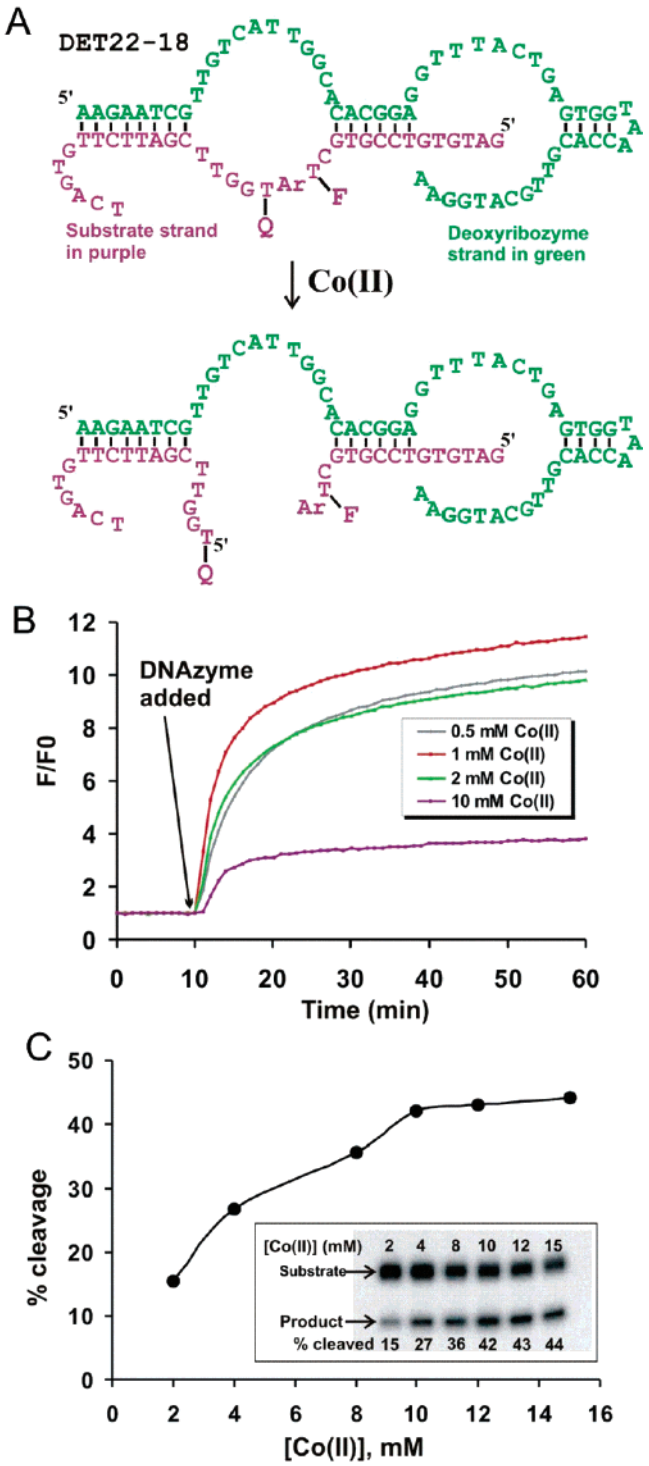

Figure 7. Effect of Co^{2+} concentrations on the signaling property and catalytic activity of the fluorescence-signaling deoxyribozyme DET22-18. (A) The design and signaling mechanism of DET22-18. The substrate is shown in purple and deoxyribozyme in green. (B) Real-time signaling of the deoxyribozyme system in the presence of various Co(II) concentrations. The substrate and Co(II) were present at beginning. Right after the 10th minute, the deoxyribozyme was added. F_0 was the initial fluorescence reading, and F was the reading at a given time point. (C) The cleavage activity of DET22-18 in the presence of various Co(II) concentrations measured by radioactivity assay. The 5′-^{32}P-phosphorylated substrate was used. The cleavage product was separated from uncleaved substrate by denaturing PAGE (embedded image). Percent cleavage is plotted versus the concentration of Co(II).

above show that the fluorescence intensity of fluorophore-tagged DNA oligonucleotides can be maximized by avoiding the use of Co(II) and Ni(II) in the selection buffer, running selections and assays at high ionic strength, and by designing aptamers and deoxyribozymes in such a way as to remove the fluorophore from G-rich or duplex regions. Ideally, removal of all transition metal cofactors would be optimal; however, to date, many catalytically efficient deoxyribozymes that have been isolated require transition metal ions as cofactors.[36,37,47] Clearly, there is a need for further investigation of the potential for isolating deoxyribozymes that can operate without transition metal ions. Ideally, such deoxyribozymes would be able to operate with Mg(II) as a cofactor since this metal ion does not cause appreciable quenching of fluorescence.

In cases where it is not possible to remove transition metal ions, or where such metal ions are likely to be present as contaminants, a second strategy that should be employed to maximize fluorescence signaling capacity is to situate the fluorescent probe in a region that is removed from either G-rich segments or duplex structures.

On the basis of the study by Atherton and Beaumont,[71] which examined the distance dependence for quenching of ethidium bromide (EB) metal ions bound to duplex DNA, we can estimate the distance from metal ions needed to maximize the fluorescence intensity (i.e., minimize quenching). In their study, using EB with an unquenched lifetime of 23 ns, electron transfer was shown to occur over 4−6 bases, based on the calculated electron transfer rate constant from EB to Co(II) in duplex DNA. Assuming that the electron transfer rate constant is similar in our system (for double-stranded DNA segments) and utilizing an unquenched lifetime of 4 ns for fluorescein, we calculate that electron transfer can occur only from adjacent nucleotides, given that electron transfer must occur over the excited-state lifetime. On the basis of this calculation, we estimate that the fluorophore must sit at least one atomic radius from a G residue or at least two residues away from the nearest G residue to minimize quenching. In such a case, the fluorescence intensity in the presence of metal ions, such as Ni(II), will be close to 20-fold higher than in the case where the probe is situated in a G-rich duplex region, allowing for use of a lower level of aptamer in each assay.

More interesting is the possibility to use the inherent sensitivity to such structural features as part of the signaling mechanism. For example, if one situates the fluorophore within a segment that has a high C content and which forms a duplex to bring a large number of G residues close to the fluorophore, a very low fluorescence background signal should be obtained. If catalysis or, in the case of aptamers, structure switching can lead to an alteration in the conformation around the probe that causes loss of the duplex structure, then significant increases in signal may result. When coupled with a secondary dequenching mechanism, such as removal of a proximal quenching moiety,[27,37] large enhancements in fluorescence signaling could be achieved. We are currently examining both selection of deoxyribozymes in the absence of transition metals and the effects of fluorophore location on signaling ability. The results of these studies will be reported in due course.

Conclusions

The proper folding and activity of signaling aptamers and signaling deoxyribozymes are often dependent upon the presence of divalent metal ions, which are required for the optimal

structural folding or catalysis. However, their inclusion must be carefully planned through the rational engineering of signaling aptamers and deoxyribozymes so that the fluorophore is tethered to a region removed from metal ion binding sites which can negatively affect fluorescence performance, or that can be removed from such a site as a consequence of target binding. Our studies have shown that rational design is necessary to avoid the excessive quenching effects that divalent transition metal ions can impose on the fluorescent system and point to a unique advantage of structure-switching aptamers: the ability to alter the fluorophore-labeled region without altering the binding site. Additionally, if possible, it is prudent to use metal ions in selection buffers that minimize quenching (Ca(II) or Mg(II)), during the evolution process, since this will result in maximum signaling efficiency for the resulting DNA aptamer. It must be noted that the choice of metals will depend on the specific application, that is, in vitro versus intracellular signaling, and that other issues, such as cytotoxicity of the metals and the presence of metal ions native to the system under study, must also be considered when optimizing the aptamer performance.

Finally, we should note that, while this study focused exclusively on quenching in DNA systems, a similar examination of quenching in fluorophore-labeled RNA is also important, given the widespread use of RNA for the development of aptamers and ribozymes. While we have no quenching data on RNA systems, we note that the high degree of similarity in both the nature of the bases and the sugar−phosphate backbone should lead to relatively similar quenching for RNA-based materials, although the presence of the 2′-hydroxyl group may provide alterations in quenching behavior. Further examination of quenching in RNA systems is thus warranted.

Acknowledgment. The authors thank MDS-Sciex, the Natural Sciences and Engineering Research Council of Canada (NSERC), the Canadian Institutes for Health Research (CIHR), the Ontario Ministry of Energy, Science and Technology, the Canada Foundation for Innovation (CFI), and the Ontario Innovation Trust (OIT) for support of this work. N.R. holds an Ontario Graduate Scholarship in Science and Technology. R.N. holds a CIHR doctoral award. Y.L. is a Canada Research Chair in Nucleic Acids Biochemistry. J.D.B. holds the Canada Research Chair in Bioanalytical Chemistry.

JA053336N